

COMMUNICATION



Cite this: *Chem. Commun.*, 2019, 55, 2469

Received 25th December 2018,
Accepted 31st January 2019

DOI: 10.1039/c8cc10203a

rsc.li/chemcomm

Enhanced electrocatalytic activity of water oxidation in an alkaline medium *via* Fe doping in CoS₂ nanosheets†

Weisu Kong, Xiaoqian Luan, Huitong Du, Lian Xia * and Fengli Qu *

The development of new electrocatalysts is critical for efficient water electrolysis to produce hydrogen. In this communication, we report a novel electrocatalyst for the oxygen evolution reaction (OER) which is realized *via* Fe doping in CoS₂ nanosheets (Fe–CoS₂). This catalyst shows an overpotential of 302 mV for a current density of 10 mA cm^{−2}, 85 mV less than that for CoS₂. In addition, Fe–CoS₂ also exhibits high catalytic stability.

The expanding energy crisis and accompanying environmental problems have boosted the exploration of clean energy.^{1,2} Electrocatalytic water splitting is regarded as a promising means to generate hydrogen and oxygen for replacing fossil fuel energy sources.^{3–7} The oxygen evolution reaction (OER), a half reaction of water splitting, occurs on the anode with sluggish kinetics due to multistep proton-coupled electron transfer.^{8,9} Consequently, it is critical to seek highly efficient electrocatalysts for the OER to make water splitting more energy-efficient. At present, noble metal oxides such as RuO₂ and IrO₂ are considered to be the best OER electrocatalysts, but the scarcity and high cost restrict their practical applications.^{8–10} Thus, it is urgently required to develop cheap and high-efficiency OER electrocatalysts.

In recent years, transition metals have been widely applied for designing electrocatalysts.^{11–14} Among these electrocatalysts, transition metal sulfides have emerged as promising OER electrocatalysts due to their high conductivity and facile fabrication processes.^{15–17} CoS₂ has been reported as an efficient alkaline OER catalyst due to its high activity.^{18,19} It has been reported that metallic element doping can enhance the catalytic performance of electrocatalysts by virtue of optimizing the hydrogen adsorption energy and enhancing electronic conductivity.^{20–24} Fe is regarded as a potential transition

metal element for designing OER electrocatalysts with a low price and adequate reserves.^{25,26} Hence, we anticipate that the OER activity of CoS₂ can be further enhanced by Fe doping to make water splitting more energy-efficient.

In this communication, we develop a novel electrocatalyst by Fe doping in CoS₂ nanosheets and supported on carbon cloth (Fe–CoS₂/CC). This catalyst presents enhanced OER performance needing an overpotential of 302 mV to afford a current density of 10 mA cm^{−2}, 85 mV less than that for CoS₂/CC. Furthermore, Fe–CoS₂/CC also shows long term stability for at least 20 h.

Fe–CoS₂/CC was derived from its hydroxide precursor *via* the hydrothermal sulfide reaction (see the ESI† for preparation details). The precursor X-ray power diffraction (XRD) pattern shows the crystallographic structure of Fe–CoS₂/CC; the diffraction peaks at 32.3°, 36.2°, 39.8°, 46.3°, 54.9°, 57.6°, 60.1°, and 62.7° can be indexed to the (200), (210), (211), (220), (311), (222), (230), and (321), planes of the CoS₂ phase (JCPDS No. 41-1471), respectively. The other peaks correspond to CC (Fig. 1a).

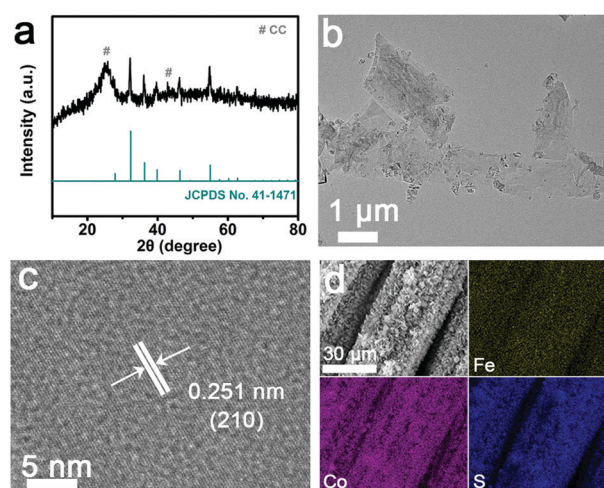


Fig. 1 (a) XRD pattern for Fe–CoS₂/CC. (b) TEM image of the Fe–CoS₂ nanosheet. (c) HRTEM image of the Fe–CoS₂ nanosheet. (d) EDX elemental mapping images of Fe, Co and S for Fe–CoS₂/CC.

College of Chemistry and Chemical Engineering, Qufu Normal University, Qufu 273165, Shandong, China. E-mail: xialian01@163.com, fengliquhn@hotmail.com

† Electronic supplementary information (ESI) available: Experimental section and supplementary figures. See DOI: 10.1039/c8cc10203a

It should be noted that no other Fe-based diffraction peaks are presented in the XRD pattern, indicating that the Fe atoms should be embedded in the atomic structure of CoS_2 as a dopant. The transmission electron microscopy (TEM) image (Fig. 1b) and the TEM figure in the sub-nano-scale (Fig. S1, ESI†) indicate the nanosheet nature of Fe- CoS_2 (Fig. 1b). A high-resolution TEM (HRTEM) image (Fig. 1c) was taken for the Fe- CoS_2 nanosheets and shows an interplanar distance of 0.251 nm, which corresponds to the (210) lattice plane of CoS_2 . As shown in Fig. 1d, the energy-dispersive X-ray (EDX) elemental mapping analysis confirms the uniform distribution of Fe, Co and S elements throughout the whole nanosheet array. As shown in Fig S2 (ESI†), the selected area electron diffraction (SAED) pattern presents two diffraction rings recorded for the Fe- CoS_2 can be ascribed to the (111) and (221) planes of CoS_2 .

The X-ray photoelectron spectroscopy (XPS) survey spectrum of Fe- CoS_2 confirms the existence of Fe, Co and S elements (Fig. 2a). In the Fe 2p region (Fig. 2b), the binding energy (BE) at 712.1 and 724.7 eV can be assigned to Fe 2p_{3/2} and Fe 2p_{1/2}, respectively.²⁷ As presented in Fig. 2c, the Co 2p region shows four peaks at 779.0, 785.8, 797.5 and 803.0 eV that can be indexed to the Co 2p_{3/2}, Co-O, Co 2p_{1/2} and Co-O, respectively.^{28,29} In the high-resolution image of Co 2p of pure CoS_2 , the Co-O peak was detected only on the low-intensity surface, and no peak of Co 2p was observed.³⁰ This phenomenon might be due to superficial cobalt oxide because CoS_2 was susceptible to oxidation in air. Fig. 2d shows the S 2p region of Fe- CoS_2 , and the wide peak in the range of 161.0–164.0 eV could be fitted into two peaks, corresponding to S 2p_{1/2} and S 2p_{3/2}. This analysis provides evidence of the presence of CoS_2 . The XPS peak at about 169.0 eV corresponded to sulfur oxide in CoS_2 (Fig. 2d).^{31,32} In pure CoS_2 , the S 2p_{1/2} and S 2p_{3/2} peaks became more obvious with higher density than the peak of S-O after Fe doping. This intensity enhancement was possibly due to the reaction of a dopant with superficial cobalt sulfate oxide of CoS_2 .³⁰ There was still oxide in Fe- CoS_2/CC due to exposure to air, which was

consistent with Sun's report.³³ It should be noted that the shifts in the values of binding energy in the XPS spectra of Fe- CoS_2 compared with pure CoS_2 indicate the presence of strong electron interactions after Fe doping, which has important implications in modulating electronic environments and thus promoting the OER activity.³⁴ The XPS analysis further indicated the successful preparation of Fe doped CoS_2 .

The OER catalytic performance of Fe- CoS_2 was calculated in 1.0 M KOH and using a standard three electrode system with a scan rate of 5 mV s⁻¹. The OER performances of bare CC, RuO_2/CC and CoS_2/CC were also measured under the same conditions for comparison. Due to the presence of ohmic potential drop (iR), the as-measured reaction currents cannot directly influence the intrinsic behavior of the catalysts.^{35–37} Accordingly, all the initial data were infrared corrected for further analysis and all data were reported on a reversible hydrogen electrode (RHE) scale. Fig. 3a shows the linear sweep voltammetry (LSV) curves of bare CC, RuO_2/CC , CoS_2/CC and Fe- CoS_2/CC . Obviously, RuO_2/CC shows excellent OER catalytic performance and only needs an overpotential of 230 mV to drive a current density of 10 mA cm⁻², whereas bare CC has almost no OER activity. As expected, Fe- CoS_2 presents superior OER activity with an overpotential of 304 mV to afford a current density of 10 mA cm⁻², 85 mV less than that for CoS_2/CC . This result indicates that the OER performance of CoS_2 can be improved obviously *via* Fe doping. It should be noted that Fe- CoS_2/CC possesses favourable behaviour compared to the other non-noble metal catalysts under alkaline conditions (Table S1, ESI†). Since commercial alkaline water electrolysis is usually carried out in a strongly alkaline medium, we also investigated the OER performance of Fe- CoS_2/CC 30 wt% KOH. As shown in Fig. S3 (ESI†), Fe- CoS_2 presented excellent OER performance needing an overpotential of 199 mV to drive a current density of 10 mA cm⁻². The reaction kinetics of the OER

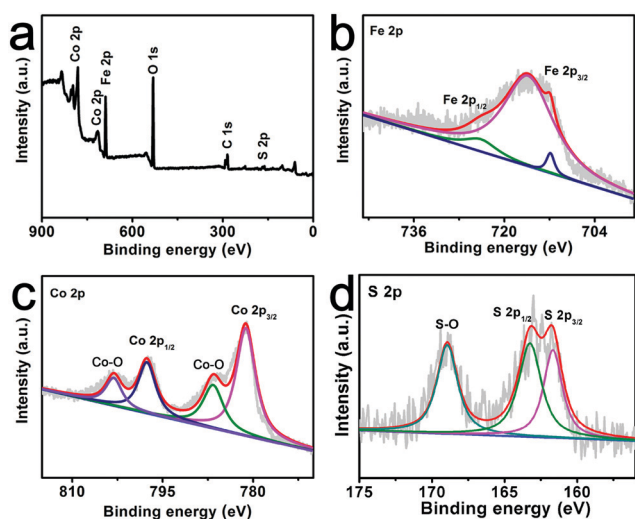


Fig. 2 (a) XPS survey spectrum for Fe- CoS_2/CC . XPS spectra in the (b) Fe 2p, (c) Co 2p and (d) S 2p regions for Fe- CoS_2/CC .

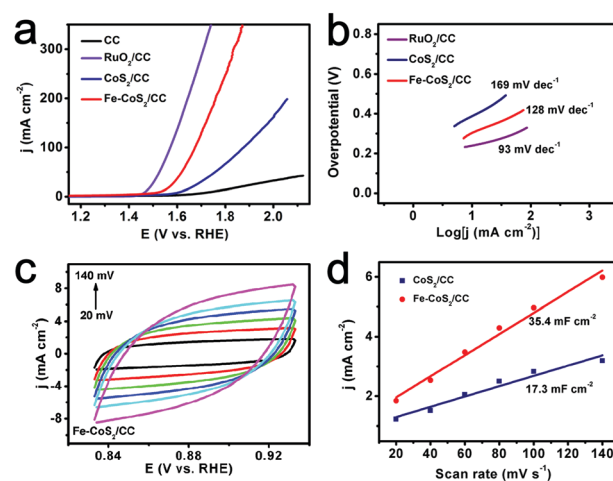


Fig. 3 (a) LSV curves of bare CC, RuO_2/CC , CoS_2/CC and Fe- CoS_2/CC with a scan rate of 5 mV s⁻¹. (b) Tafel plots of RuO_2/CC , CoS_2/CC and Fe- CoS_2/CC . (c) CVs of Fe- CoS_2/CC with various scan rates. (d) Capacitive currents at 0.88 V as a function of the scan rate for CoS_2/CC and Fe- CoS_2/CC .

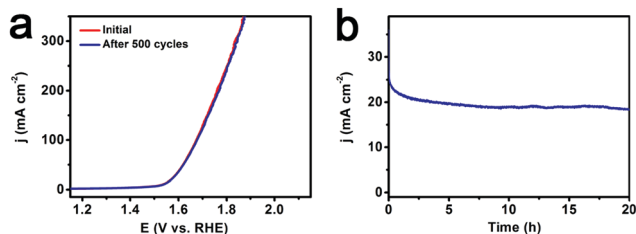


Fig. 4 (a) LSV curves for Fe–CoS₂/CC before and after 500 CV cycles. (b) Time-dependent current density curve of Fe–CoS₂/CC at a static overpotential of 340 mV.

can be estimated by the Tafel equation: $\eta = b \log j + a$, where b is the Tafel slope and j is the current density.³⁸ As shown in Fig. 3b, the Tafel plots for RuO₂/CC, CoS₂/CC and Fe–CoS₂/CC were plotted. RuO₂/CC exhibits a Tafel slope of 93 mV dec⁻¹. In addition, Fe–CoS₂/CC shows a Tafel slope value of 128 mV dec⁻¹, lower than that of CoS₂/CC (169 mV dec⁻¹), implying faster OER kinetics of Fe–CoS₂/CC and the intrinsic catalytic activity of CoS₂ can be enhanced by Fe doping. Furthermore, to verify that this Fe-doping effect also applied to other substances, we performed this work on Ti mesh (TM), and the OER performance of CoS₂ also shows improvement after Fe doping (Fig. S4, ESI[†]). To reveal the improved OER activity of CoS₂/CC by Fe doping, the double layer capacitances (C_{dl}) of CoS₂/CC and Fe–CoS₂/CC were calculated based on the cyclic voltammograms (CVs) at different scan rates (Fig. S5, ESI[†] and Fig. 3c). As shown in Fig. 3d, the C_{dl} value of Fe–CoS₂/CC (35.4 mF cm⁻²) is larger than that of CoS₂/CC (17.3 mF cm⁻²), implying a higher surface roughness and that more active sites were exposed for Fe–CoS₂/CC, which is in favor of the enhanced OER performance.^{39–42} Fig. S6 (ESI[†]) shows a multi-step chronopotentiometric curve for Fe–CoS₂/CC in 1.0 M KOH with the current density being increased from 20 to 200 mA cm⁻² (20 mA per cm⁻² per 500 s). The potential is instantaneously stabilized at an initial current value of 1.61 V and remains constant for the remaining 500 s and other steps showed similar results, suggesting that the Fe–CoS₂/CC possesses excellent electrical conductivity, mechanical strength and mass transfer ability.^{43,44}

In addition, the stability is another important parameter for evaluating the performances of electrocatalysts. Thus, we investigated the stability of Fe–CoS₂/CC using CV technology. As plotted in Fig. 4a, the Fe–CoS₂/CC only shows a slight loss in the current density after 500 CV cycles, suggesting the good stability of the catalyst. Furthermore, we also performed the OER at a static overpotential of 340 mV and the Fe–CoS₂/CC presents superior long term stability and maintains its catalytic activity for at least 20 h (Fig. 4b). Based on the above investigations, the enhanced OER performance of CoS₂ by Fe doping can be attributed to the following reasons: (i) a synergistic effect may be created by Fe doping,^{45–47} and (ii) the improved surface roughness and exposure of more activity sites.^{48–51}

In summary, the enhanced OER catalytic activity of CoS₂/CC via Fe doping was proven experimentally. This Fe–CoS₂/CC shows efficient OER catalytic activity needing an overpotential of 302 mV to afford a current density of 10 mA cm⁻², 85 mV less than that for CoS₂/CC. In addition, this catalyst also possesses

superior durability and maintains its catalytic properties for at least 20 h. This work not only provides us with an attractive and cost-efficient catalyst for electrochemical water oxidation in alkaline media, but also provides important guidance for designing and synthesizing CoS₂-based catalysts with enhanced OER activity.

This work was supported by the National Natural Science Foundation of China (21775089 and 21505084), the Outstanding Youth Foundation of Shandong Province (ZR2017JL010), the Natural Science Foundation Projects of Shandong Province (ZR2014BM029), and the Key Research and Development Program of Jining City (2018ZDGH032).

Conflicts of interest

There are no conflicts to declare.

References

- H. Wu, B. Xia, L. Yu, X. Yu and X. Lou, *Nat. Commun.*, 2015, **6**, 6512.
- H. Gray, *Nat. Commun.*, 2009, **1**, 7.
- B. Chen, Z. Jiang, J. Huang, B. Deng, L. Zhou, Z. Jiang and M. Liu, *J. Mater. Chem. A*, 2018, **6**, 9517–9527.
- Z. Khan, S. Park, J. Yang, S. Park, R. Shanker, H. Song, Y. Kim, S. Kwak and H. Ko, *J. Mater. Chem. A*, 2018, **6**, 24459–24467.
- Z. Khan, S. Park, S. Hwang, J. Yang, Y. Lee, H. Song, Y. Kim and H. Ko, *NPG Asia Mater.*, 2016, **8**, e294.
- L. Zhou, B. Deng, Z. Jiang and Z. Jiang, *Chem. Commun.*, 2019, **55**, 525–528.
- H. Du, X. Zhang, Q. Tan, R. Kong and F. Qu, *Chem. Commun.*, 2017, **53**, 12012–12015.
- S. Xue, L. Chen, Z. Liu, H. Cheng and W. Ren, *ACS Nano*, 2012, **6**, 5297–5305.
- X. Zhang, C. Si, X. Guo, R. Kong and F. Qu, *J. Mater. Chem. A*, 2017, **5**, 17211–17215.
- X. Zhang, W. Sun, H. Du, R. Kong and F. Qu, *Inorg. Chem. Front.*, 2018, **5**, 344–347.
- Y. Hou, Y. Liu, R. Gao, Q. Li, H. Guo, A. Goswami, R. Zboril, M. Gawander and X. Zou, *ACS Catal.*, 2017, **7**, 7038–7042.
- Z. Wang, Z. Liu, G. Du, A. Asiri, L. Wang, X. Li, H. Wang, X. Sun, L. Chen and Q. Zhang, *Chem. Commun.*, 2018, **54**, 810–813.
- Z. Wang, X. Ren, X. Shi, A. M. Asiri, L. Wang, X. Li, X. Sun, Q. Zhang and H. Wang, *J. Mater. Chem. A*, 2018, **6**, 3864–3868.
- H. Du, R. Kong, F. Qu and L. Lu, *Chem. Commun.*, 2018, **54**, 10100–10103.
- W. Zhu, X. Yue, W. Zhang, S. Yu, Y. Zhang, J. Wang and J. Wang, *Chem. Commun.*, 2016, **52**, 1486–1489.
- I. Chen, J. Ren, M. Shalom, T. Fellerger and M. Antonietti, *ACS Appl. Mater. Interfaces*, 2016, **8**, 5509–5516.
- D. Xiong, Q. Zhang, W. Li, J. Li, X. Fu, M. Cerqueira, P. Alpuim and L. Liu, *Nanoscale*, 2017, **9**, 2711–2717.
- X. Han, X. Wu, Y. Deng, J. Liu, C. Zhong and W. Hu, *Adv. Energy Mater.*, 2018, **8**, 1800935.
- X. Ma, W. Zhang, Y. Deng, C. Zhong, W. Hu and X. Han, *Nanoscale*, 2018, **10**, 4816–4824.
- T. Liu, D. Liu, F. Qu, D. Wang, L. Zhang, R. Ge, S. Hao, Y. Ma, G. Du, A. Asiri, L. Chen and X. Sun, *Adv. Energy Mater.*, 2017, **7**, 1700020.
- H. Du, L. Xia, S. Zhu, F. Qu and F. Qu, *Chem. Commun.*, 2018, **54**, 2894–2897.
- D. Wang, M. Gong, H. Chou, C. Pan, H. Chen, Y. Wu, M. Lin, M. Guan, J. Yang, C. Chen, Y. Wang, B. Hwang, C. Chen and H. Dai, *J. Am. Chem. Soc.*, 2015, **137**, 1587–1592.
- R. Zhang, C. Tang, R. Kong, G. Du, A. M. Asiri, L. Chen and X. Sun, *Nanoscale*, 2017, **9**, 4793–4800.
- T. Liu, A. M. Asiri and X. Sun, *Nanoscale*, 2016, **8**, 3911–3915.
- C. Tang, R. Zhang, W. Lu, L. He, X. Jiang, A. Asiri and X. Sun, *Adv. Mater.*, 2017, **29**, 1602441.

- 26 X. Guo, S. Zhu, R. Kong, X. Zhang and F. Qu, *ACS Sustainable Chem. Eng.*, 2018, **6**, 1545–1549.
- 27 M. M. R. Dedryvère, L. Croguennec, F. Le Cras, C. Delmas and D. Gonbeau, *Chem. Mater.*, 2008, **20**, 7164–7170.
- 28 C. Ouyang, X. Wang and S. Wang, *Chem. Commun.*, 2015, **51**, 14160–14163.
- 29 M. S. Faber, R. Dziejic, M. A. Lukowski, N. S. Kaiser, Q. Ding and S. Jin, *J. Am. Chem. Soc.*, 2014, **136**, 10053–10061.
- 30 C. Ouyang, X. Wang and S. Wang, *Chem. Commun.*, 2015, **51**, 14160–14163.
- 31 H. Zhang, Y. Li, G. Zhang, T. Xu, P. Wan and X. Sun, *J. Mater. Chem. A*, 2015, **3**, 6306–6310.
- 32 X. Guo, R. Kong, X. Zhang, H. Du and F. Qu, *ACS Catal.*, 2018, **8**, 651–655.
- 33 Q. Liu, J. Tian, W. Cui, P. Jiang, N. Cheng, A. M. Asiri and X. Sun, *Angew. Chem.*, 2014, **126**, 6828–6832.
- 34 S. Wei, X. Wang, J. Wang, X. Sun, L. Cui, W. Yang, Y. Zheng and J. Liu, *Electrochim. Acta*, 2017, **246**, 776–782.
- 35 Q. Zhang, P. Li, D. Zhou, Z. Chang, Y. Kuang and X. Sun, *Small*, 2017, **13**, 1701648.
- 36 H. Du, X. Guo, R. Kong and F. Qu, *Chem. Commun.*, 2018, **54**, 12848–12851.
- 37 H. Du, L. Xia, S. Zhu, F. Qu and F. Qu, *Chem. Commun.*, 2018, **54**, 2894–2897.
- 38 P. Jiang, Q. Liu, Y. Liang, J. Tian, A. M. Asiri and X. Sun, *Angew. Chem., Int. Ed.*, 2014, **53**, 12855–12859.
- 39 H. Du, R. Kong, X. Guo, F. Qu and J. Li, *Nanoscale*, 2018, **10**, 21617–21624.
- 40 S. Hao, L. Yang, D. Liu, R. Kong, G. Du, A. M. Asiri, Y. Yang and X. Sun, *Chem. Commun.*, 2017, **53**, 5710–5713.
- 41 C. C. L. McCrory, S. Jung, J. C. Peters and T. F. Jaramillo, *J. Am. Chem. Soc.*, 2013, **135**, 16977–16987.
- 42 F. Yu, H. Yao, B. Wang, K. Zhang, Z. Zhang, L. Xie, J. Hao, B. Mao, H. Shen and W. Shi, *Dalton Trans.*, 2018, **47**, 9871–9876.
- 43 X. Lu and C. Zhao, *Nat. Commun.*, 2015, **6**, 6616.
- 44 L. Cui, D. Liu, S. Hao, F. Qu, G. Du, J. Liu, A. M. Asiri and X. Sun, *Nanoscale*, 2017, **9**, 3752–3756.
- 45 Y. Zhang, Y. Liu, M. Ma, X. Ren, Z. Liu, G. Du, A. M. Asiri and X. Sun, *Chem. Commun.*, 2017, **53**, 11048–11051.
- 46 A. Wang, J. Lin, H. Xu, Y. Tong and G. Li, *J. Mater. Chem. A*, 2016, **4**, 16992–16999.
- 47 L. Xie, F. Qu, Z. Liu, X. Ren, S. Hao, R. Ge, G. Du, A. M. Asiri, X. Sun and L. Chen, *J. Mater. Chem. A*, 2017, **5**, 7806–7810.
- 48 Y. Zhu, C. Su, X. Xu, W. Zhou, R. Ran and Z. Shao, *Chem. – Eur. J.*, 2014, **20**, 15533–15542.
- 49 X. Long, G. Li, Z. Wang, H. Zhu, T. Zhang, S. Xiao, W. Guo and S. Yang, *J. Am. Chem. Soc.*, 2015, **137**, 11900–11903.
- 50 H. Zhang, Y. Li, T. Xu, J. Wang, Z. Huo, P. Wan and X. Sun, *J. Mater. Chem. A*, 2015, **3**, 15020–15023.
- 51 Z. Xing, Q. Liu, A. M. Asiri and X. Sun, *Adv. Mater.*, 2014, **26**, 5702–5707.